ChemCatChem

Research Article
doi.org/10.1002/cctc.202201007

Chemistry Europe
European Chemical Societies Publishing

www.chemcatchem.org

Constrained Geometry *ansa*-Half-Sandwich Complexes of Magnesium – Versatile *s*-Block Catalysts

Lisa Wirtz,[a] Kinza Yasmin Ghulam,[a] Bernd Morgenstern,[a] and André Schäfer*[a]

The synthesis, characterization and catalytic application of a series of constrained geometry *ansa*-half-sandwich complexes of magnesium is reported. These versatile *s*-block catalysts were applied in different dehydrocoupling and hydroelementation reactions, demonstrating a broad applicability with particularly remarkable performance in dehydrocoupling reactions.

Introduction

ansa-Half-sandwich ligands are quite popular in transition metal chemistry.[1–4] For example, complexes of group 3 and 4 metals have been known since the early 1990s and are often used in homogenous catalysis, such as olefin polymerization, and are even applied in industrial processes.[3,5,6] Different types of these so-called constrained geometry catalysts (CGCs) are known, which exhibit different *ansa* bridging motifs and various cyclopentadienyl, indenyl or fluorenyl groups.[3,7] In contrast, such *ansa*-half-sandwich ligands have only rarely found application in main-group chemistry.[8–10] In 2001 and 2003, Cowley and coworkers reported constrained geometry *ansa*-half-sandwich complexes of group 13 and group 15 compounds, followed by a report from our group about related heavy group 14 *N*-heterocyclic half-sandwich complexes.[8,9,11] The first constrained geometry alkaline earth metal complex of this type, containing calcium as the central atom, was reported by Tamm and coworkers in 2008.[12] Subsequently, magnesium complexes of this type have also been described, but – until now – have not been structurally authenticated, and in general, such constrained geometry *ansa*-half-sandwich complexes of main group elements have seen only little application in homogenous catalysis.[10,13]

In general, the interest in *s*-block based catalysts has grown tremendously over the past decades,[14–16] due to the attractive properties of these metals for catalytic applications, which are their high natural abundances in the earth's crust, their associated low carbon footprint and their low toxicity, high biocompatibility respectively.[17,18] Thus, there is considerable interest in magnesium based catalysts with a broad applicability spectrum, and since magnesium can be considered a "green" metal in catalysis for the afore mentioned reasons, transformations with no or minimal by-product are of particular interest. One such reaction type for the formation of new E–E bonds (E = *p*-block element) with a particularly high atom economy is dehydrocoupling, which generates dihydrogen as the only by-product, while providing easy and straight forward access to a number of inorganic *p*-block compounds.[19–23] There are several examples of such reactions catalyzed by magnesium. For instance, magnesium compounds have been employed in dehydrocoupling reactions of amine-boranes,[24–29] and in cross-dehydrocoupling reactions of amines with silanes.[25,30–32] Furthermore, magnesium-based catalysts have also been employed in hydroelementation reactions, pioneered by the groups of Hill, Harder, Sadow and others.[15,33] For example, magnesium-catalyzed hydroborations are a well-established area[14,33–38] as is the important reaction type of hydroamination, such as intramolecular ring-closing hydroamination for the preparation of *N*-heterocycles.[13,39–47] Furthermore, interest in atom-economical C–C bond formation in organic chemistry has increased. The field was formerly dominated by transition metal catalysts, but more recently, main group and in particular *s*-block based catalysts are now being established.[48,49]

Inspired by these aspects and our continued interest in main-group Cp complexes and their application in homogenous catalysis, we were intrigued to develop a magnesium-based catalyst system that could be employed in a wide variety of reaction types. Herein, we report the syntheses and characterization of four constrained geometry *ansa*-half-sandwich complexes of magnesium and their versatile applications as catalysts in different dehydrocoupling and hydroelementation reactions.

Results and Discussion

Synthesis and Characterization of *ansa*-Half-Sandwich Magnesium Complexes

Literature known *ansa*-half-sandwich ligands[50–53] were reacted with dibutylmagnesium to obtain the corresponding *ansa*-half-sandwich magnesium complexes **1a–d** (Scheme 1). Similar to

[a] L. Wirtz, K. Y. Ghulam, Dr. B. Morgenstern, Dr. A. Schäfer
Faculty of Natural Science and Technology
Department of Chemistry
Saarland University
Campus Saarbrücken
66123 Saarbrücken (Germany)
E-mail: andre.schaefer@uni-saarland.de

Supporting information for this article is available on the WWW under https://doi.org/10.1002/cctc.202201007

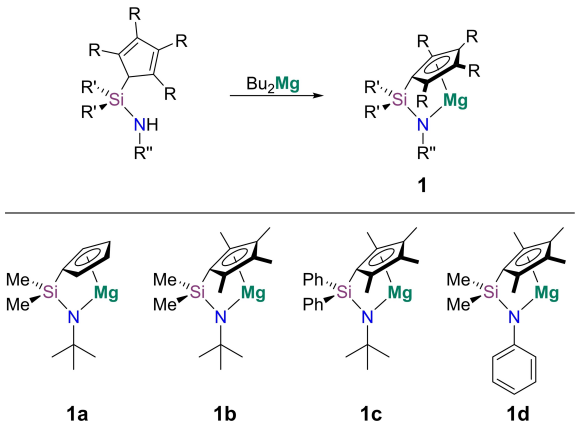

Scheme 1. Synthesis of magnesium complexes **1 a**–**d**.

magnesocenophanes,[24,25,54–56] **1 a**–**d** possess Lewis acidic magnesium atoms and crystalized as solvent adducts from donor solvent (Figure 1, S14–S18). In case of **1 a**–**c**, mono dme adducts are observed in the solid state, with the dme molecule coordinated to the magnesium atom *via* both oxygen atoms and the magnesium atom exhibiting an η^5 coordination mode to the Cp group. In case of *N*-phenyl complex **1 d**, two dme molecules are coordinated to the magnesium atom in the solid state, with one bonded *via* both and one only *via* one oxygen atom. Consequently, the magnesium atom exhibits an η^1 coordination to the Cp ligand. Although this solid-state structure does not necessarily reflect the situation in solution, it highlights the coordinative flexibility of this Cp-based ligand system, which can adopt to and compensate for the electronic and steric situation at the central atom. Noteworthy, similar η^1 ring slippage structures were observed for [1]magnesocenophane thf and amine complexes in the past.[24,25,57]

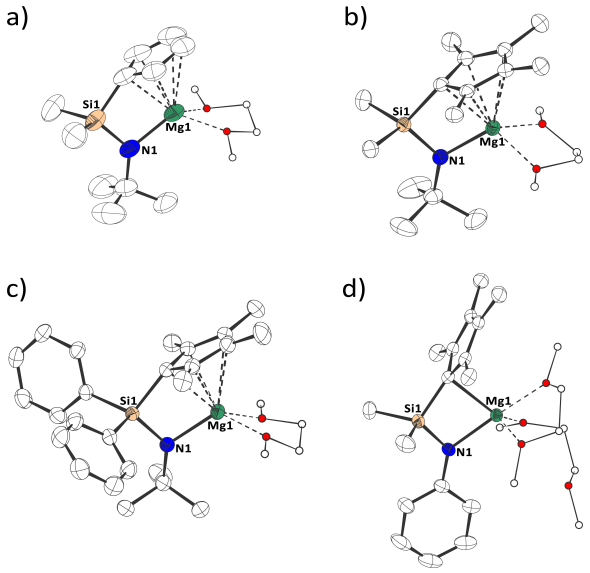

Figure 1. Molecular structures of a) **1 a**·dme, b) **1 b**·dme, c) **1 c**·dme, and d) **1 d**·$(dme)_2$ in the crystal (displacement ellipsoids for 50% probability level; hydrogen atoms omitted for clarity; dme molecules drawn as ball-and-stick models).

The Mg–O^{dme} bonds are 203.98(41) to 210.66(11) pm, which is slightly longer than the Mg–O^{thf} bonds in **1 a**·$(thf)_2$ (202.67(31) to 204.98(33) pm; Table S1) and in line with what was previously observed in dme and thf adducts of [1]magnesocenophanes.[24,25] Corresponding to this, DFT calculations indicate stronger binding of thf than dme (Table S2).[24,25,57] The Mg–Cp^{cent} bond distances in **1 a**–**c**·(dme) are 215.05(6) to 220.36(7) pm (Table S1), which is again similar to the distances in dme complexes of [1]magnesocenophanes. Regarding electronic properties, DFT calculations predict fluoride ion affinities (FIA)[58] and global electrophilicity indices (GEI),[59] slightly below those for previously reported [1]magnesocenophanes, but still indicate a pronounced Lewis acidic character of the magnesium center.[24,60]

Dehydrocoupling Catalysis

Amine-Borane Dehydrocoupling

Recently, we demonstrated that [1]magnesocenophanes are potent catalysts in the dehydrocoupling of amine-boranes.[24,25] While many magnesium based catalysts require elevated temperatures to operate,[26–29] [1]magnesocenophanes were able to catalyze the dehydrocoupling reactions of different dialkylamine-boranes at room temperature.[24,25] We therefore started our investigations into the catalytic abilities of *ansa*-half-sandwich magnesium complexes **1 a**–**d** by testing their performance in the dehydrocoupling of amine-boranes. The dehydrocoupling of dimethylamine-borane to cyclic tetramethyldiborazane takes place at room temperature with 5 mol% of **1 a**–**d**, giving up to 87% conversion after just 8 h. Analogously, the dehydrocoupling of piperidine-borane, morpholine-borane and di*iso*propylamine-borane gave quantitative or near quantitative conversions with 5 mol% of **1 a**–**d** after 8 h at room temperature (Scheme 2; Table 1).

This is significantly faster than the previously reported [1]magnesocenophane-catalyzed reactions, which required approx. twice the reaction time to attain similar conversions, and by far the best performance for a magnesium catalyst.[26–29] After these promising results, we choose to expand the substrate scope and investigate the intermolecular dehydrocoupling of amines with pinacolborane, for which only few metal catalysts have been reported so far.[61–68] Since it is well known that such reaction can also occur without any catalyst in some cases,[69] we carried out control experiments with pinacolborane and the corresponding amines in the absence of any metal catalyst. Pinacolborane and *tert*-butylamine respectively pyrrolidine were stirred in dme at room temperature for 1 h, whereupon ~20% of the respective dehydrocoupling products were observed by ^{11}B NMR spectroscopy. The corresponding control experiment between *p*-toluidine and pinacolborane gave a conversion of ~50%. Following these blank experiments, *tert*-butylamine, pyrrolidine and *p*-toluidine were reacted with pinacolborane in

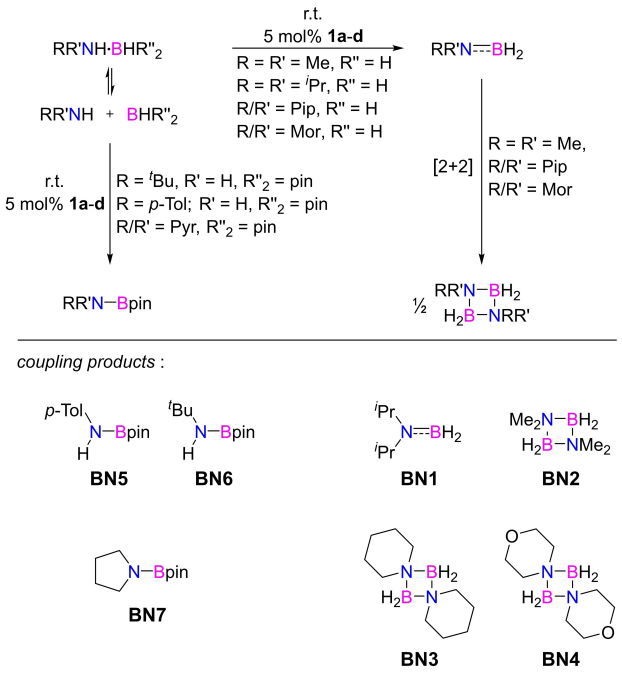

Scheme 2. Amine-borane dehydrocoupling catalyzed by **1 a–d**.

dme for 1 h in the presence of 5 mol% of **1 a–d**. This addition of 5 mol% catalyst resulted in the doubling to quadrupling of the conversions under identical reaction conditions, thus a strong catalytic effect could be observed (Scheme 2; Table 1).

Overall, this is roughly on a par with a β-diketiminato magnesium system reported by Hill and coworkers,[62] and somewhat faster than alkali-metal amide catalysts, reported by Panda and coworkers.[63] Interestingly, **1 a–d** all performed relatively similarly in the dehydrocoupling of dialkylamine-boranes and amines with pinacolborane, indicating no strong effects of the different substitution patterns on the catalytic performance. Mechanistically we assume that the amine-borane dehydrogenation/dehydrocoupling reactions catalyzed by **1 a–d** follow a similar pathway as with the related magnesocenophane systems, previously reported.[24,25]

Amine Silane Cross-Dehydrocoupling

Recently, we reported the utilization of C-[1]magnesocenophanes in amine silane cross-dehydrocoupling.[25] Therefore, following the successful application of the title compounds **1 a–d** in amine-borane dehydrocoupling, we expanded the substrate scope to silanes and investigate the possibility for catalytic Si–N bond formations. Remarkably, the cross-dehydrocoupling between diphenylsilane and methylphenylsilane with different primary and secondary amines with 5 mol% of catalyst loading, gave quantitative or near quantitative conversions in most cases after just 1 h at room temperature (Scheme 3, Table 2). Only the cross-dehydrocoupling of *tert*-butylamine and dibenzylamine with diphenylsilane yielded lower conversions, or required longer reaction

Table 1. Summary of catalysts, substrates, formed coupling products and conversions of the amine-borane dehydrocoupling reactions catalyzed by **1 a–d**, corresponding to Scheme 2.[a]

catalyst	substrate(s)	product	conversion
1 a	$^{i}Pr_2NH\cdot BH_3$	**BN1**	≥95 %
1 b·dme	$^{i}Pr_2NH\cdot BH_3$	**BN1**	≥95 %
1 c·dme	$^{i}Pr_2NH\cdot BH_3$	**BN1**	≥95 %
1 d·dme	$^{i}Pr_2NH\cdot BH_3$	**BN1**	≥95 %
1 a	$Me_2NH\cdot BH_3$	**BN2**	82 %
1 b·dme	$Me_2NH\cdot BH_3$	**BN2**	87 %
1 c·dme	$Me_2NH\cdot BH_3$	**BN2**	80 %
1 d·dme	$Me_2NH\cdot BH_3$	**BN2**	78 %
1 a	PipNH·BH_3	**BN3**	≥95 %
1 b·dme	PipNH·BH_3	**BN3**	91 %
1 c·dme	PipNH·BH_3	**BN3**	87 %
1 d·dme	PipNH·BH_3	**BN3**	≥95 %
1 a	MorNH·BH_3	**BN4**	≥95 %
1 b·dme	MorNH·BH_3	**BN4**	≥95 %
1 c·dme	MorNH·BH_3	**BN4**	91 %
1 d·dme	MorNH·BH_3	**BN4**	92 %
–	*p*-TolNH + HBpin	**BN5**	50 %
1 a	*p*-TolNH + HBpin	**BN5**	≥95 %
1 b·dme	*p*-TolNH + HBpin	**BN5**	≥95 %
1 c·dme	*p*-TolNH + HBpin	**BN5**	≥95 %
1 d·dme	*p*-TolNH + HBpin	**BN5**	≥95 %
–	$^{t}BuNH_2$ + HBpin	**BN6**	19 %
1 a	$^{t}BuNH_2$ + HBpin	**BN6**	67 %
1 b·dme	$^{t}BuNH_2$ + HBpin	**BN6**	70 %
1 c·dme	$^{t}BuNH_2$ + HBpin	**BN6**	76 %
1 d·dme	$^{t}BuNH_2$ + HBpin	**BN6**	48 %
–	PyrNH + HBpin	**BN7**	20 %
1 a	PyrNH + HBpin	**BN7**	94 %
1 b·dme	PyrNH + HBpin	**BN7**	95 %
1 c·dme	PyrNH + HBpin	**BN7**	≥95 %
1 d·dme	PyrNH + HBpin	**BN7**	72 %

[a] Conditions: **BN1–BN4**: dme; room temperature; 8 h; 5 mol% catalyst loading; **BN5–BN7**: dme; room temperature; 1 h; 5 mol% catalyst loading.

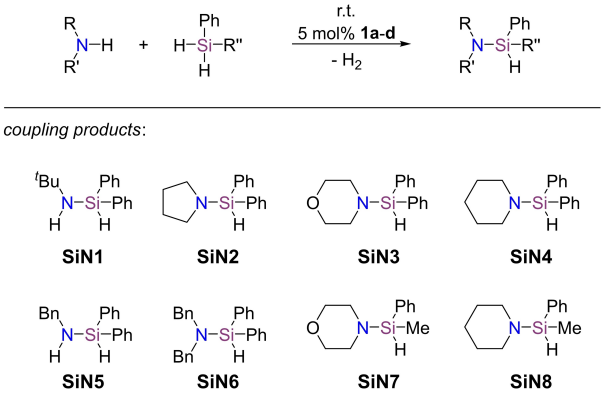

Scheme 3. Amine silane cross-dehydrocoupling catalyzed by **1 a–d**.

times respectively, presumable due to the higher steric demand of those amines. Furthermore, catalysts **1 a–d** performed relatively equally in case of **SiN2**,**3**,**4**,**5**,**7**,**8**, while **1 a** and **1 d** showed lower catalytic performance in the afore mentioned

Table 2. Summary of catalysts, substrates, formed coupling products and conversions of the amine silane cross-dehydrocoupling reactions catalyzed by **1 a–d**, corresponding to Scheme 3.[a]

catalyst	substrates	product	conversion
1 a	^{t}BuNH$_2$/Ph$_2$SiH$_2$	**SiN1**	50 %
1 b·dme	^{t}BuNH$_2$/Ph$_2$SiH$_2$	**SiN1**	65 %
1 c·dme	^{t}BuNH$_2$/Ph$_2$SiH$_2$	**SiN1**	66 %
1 d·dme	^{t}BuNH$_2$/Ph$_2$SiH$_2$	**SiN1**	31 %
1 a	PyrNH/Ph$_2$SiH$_2$	**SiN2**	≥95 %
1 b·dme	PyrNH/Ph$_2$SiH$_2$	**SiN2**	≥95 %
1 c·dme	PyrNH/Ph$_2$SiH$_2$	**SiN2**	≥95 %
1 d·dme	PyrNH/Ph$_2$SiH$_2$	**SiN2**	≥95 %
1 a	MorNH/Ph$_2$SiH$_2$	**SiN3**	≥95 %
1 b·dme	MorNH/Ph$_2$SiH$_2$	**SiN3**	≥95 %
1 c·dme	MorNH/Ph$_2$SiH$_2$	**SiN3**	≥95 %
1 d·dme	MorNH/Ph$_2$SiH$_2$	**SiN3**	≥95 %
1 a	PipNH/Ph$_2$SiH$_2$	**SiN4**	≥95 %
1 b·dme	PipNH/Ph$_2$SiH$_2$	**SiN4**	≥95 %
1 c·dme	PipNH/Ph$_2$SiH$_2$	**SiN4**	≥95 %
1 d·dme	PipNH/Ph$_2$SiH$_2$	**SiN4**	≥95 %
1 a	BnNH$_2$/Ph$_2$SiH$_2$	**SiN5**	89 %
1 b·dme	BnNH$_2$/Ph$_2$SiH$_2$	**SiN5**	92 %
1 c·dme	BnNH$_2$/Ph$_2$SiH$_2$	**SiN5**	89 %
1 d·dme	BnNH$_2$/Ph$_2$SiH$_2$	**SiN5**	≥95 %
1 a	Bn$_2$NH/Ph$_2$SiH$_2$	**SiN6**	51 %
1 b·dme	Bn$_2$NH/Ph$_2$SiH$_2$	**SiN6**	87 %
1 c·dme	Bn$_2$NH/Ph$_2$SiH$_2$	**SiN6**	88 %
1 d·dme	Bn$_2$NH/Ph$_2$SiH$_2$	**SiN6**	0 %
1 a	MorNH/MePhSiH$_2$	**SiN7**	≥95 %
1 b·dme	MorNH/MePhSiH$_2$	**SiN7**	≥95 %
1 c·dme	MorNH/MePhSiH$_2$	**SiN7**	≥95 %
1 d·dme	MorNH/MePhSiH$_2$	**SiN7**	≥95 %
1 a	PipNH/MePhSiH$_2$	**SiN8**	≥95 %
1 b·dme	PipNH/MePhSiH$_2$	**SiN8**	≥95 %
1 c·dme	PipNH/MePhSiH$_2$	**SiN8**	≥95 %
1 d·dme	PipNH/MePhSiH$_2$	**SiN8**	≥95 %

[a] Conditions: **SiN1–SiN5**,**SiN7**,**SiN8**: C_6D_6; room temperature; 1 h; 5 mol% catalyst loading; **SiN6**: C_6D_6; room temperature; 16 h; 5 mol% catalyst loading.

coupling reaction yielding **SiN1** and **SiN6**. Particularly surprise is the fact that **1 d** repeatedly and reproducibly gave almost no coupling product **SiN6** in the reaction of dibenzylamine with diphenylsilane. To preclude that this originates from poor solubility of **1 d**·dme, we repeated the reaction in thf under otherwise identical conditions, but still only observed 10 % conversion. Increased reaction times of up to 24 h and increased catalyst loadings of 10 mol% did not yield significantly higher conversions. The reason for this remains unclear, but it might be more related to electronic that steric reasons. In all cases, catalysts **1 a–d** gave selectively the mono coupling products, but no diaminosilanes and/or disilylamines.

While several magnesium-based systems are known to catalyze amine silane cross-dehydrocoupling reactions at room temperature, they typically require reaction times of 15 h to 24 h.[30–32] Thus, the performance of **1 a–d** is quite remarkable, as they give near quantitative conversions after just 1 h in many cases. Although, some heavier alkaline earth metal compounds do catalyze the cross-dehydrocoupling of amines and silanes more efficiently,[70,71] *ansa*-half-sandwich magnesium complexes **1 a–d**, in particular **1 b** and **1 c**, are among the most potent magnesium-based catalysts for amine silane cross-dehydrocoupling.

As the *ansa*-half-sandwich complexes **1 a–d** are structural related to [1]magnesocenophanes, we assume that the mechanism is similar to what we suggested before, based on experimental and theoretical investigations.[25] Most likely, the initial step involves the formation of a bis(amine) complex of the type **1 a–d**·(amine)$_2$. Such a complex could be observed spectroscopically, when **1 a** was treated with two equivalents of pyrrolidine, giving **1 a**·(pyrrolidine)$_2$.[60] Most importantly, no formation of free ligand was detected by ^{1}H/^{13}C{^{1}H}/^{29}Si{^{1}H} NMR spectroscopy in this experiment, indicating that no metal-ligands cleavage takes place and that **1 a**, **1 a**·(pyrrolidine)$_2$ respectively, is most likely involved in the catalysis and that **1 a** is not just a precatalyst. Furthermore, addition of two equivalents of diphenylsilane to this magnesium amine complex, resulted in dehydrocoupling and formation of coupling product **SiN2**, while magnesium complex **1 a** remained intact.

Hydroelementation Catalysis

Hydroboration

In general, hydroelementation reactions are of great interest for a variety of reasons, including the synthetically straight forward possibility to incorporate functional group across different unsaturated chemical bonds, combined with their high atom economy. One of the most popular hydroelementation reactions are hydroborations, for which different magnesium-based catalysts have been reported in the past.[14,33–38] Accordingly, we probed the possibility of using *ansa*-half-sandwich complexes **1 a–d** as catalysts for hydroboration reactions of alkynes, nitriles and imines with pinacolborane (Scheme 4; Table 3).

A catalyst loading of 5 mol% is commonly reported in literature[14,33,72,73] and has also been used successfully for dehydrocoupling reactions with **1 a–d**, which is why we performed our investigation with this loading. The hydro-

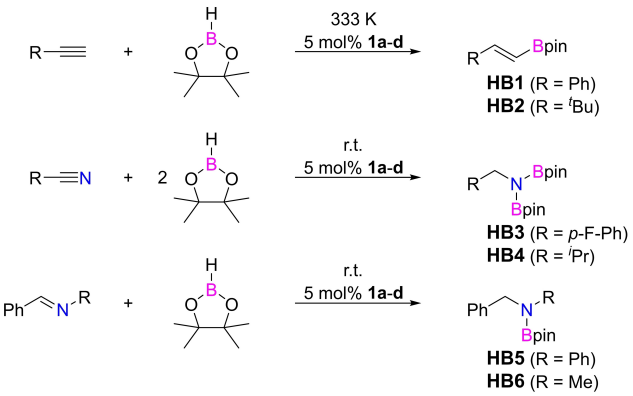

Scheme 4. Hydroboration of alkynes, nitriles and imines catalyzed by **1 a–d**.

Table 3. Summary of catalysts, substrates, formed hydroboration products and conversions of the hydroboration reactions catalyzed by **1a–d**, corresponding to Scheme 4.[a]

catalyst	substrate + n HBpin	product	conversion
–	PhC≡CH (n = 1)	**HB1**	0%
$MgBr_2$	PhC≡CH (n = 1)	**HB1**	0%
1a	PhC≡CH (n = 1)	**HB1**	81%
1b·dme	PhC≡CH (n = 1)	**HB1**	62%
1c·dme	PhC≡CH (n = 1)	**HB1**	64%
1d·dme	PhC≡CH (n = 1)	**HB1**	75%
–	^{t}BuC≡CH (n = 1)	**HB2**	4%
$MgBr_2$	^{t}BuC≡CH (n = 1)	**HB2**	20%
1a	^{t}BuC≡CH (n = 1)	**HB2**	81%
1b·dme	^{t}BuC≡CH (n = 1)	**HB2**	76%
1c·dme	^{t}BuC≡CH (n = 1)	**HB2**	88%
1d·dme	^{t}BuC≡CH (n = 1)	**HB2**	79%
–	*p*-F-PhC≡N (n = 2)	**HB3**	0%
$MgBr_2$	*p*-F-PhC≡N (n = 2)	**HB3**	0%
1a	*p*-F-PhC≡N (n = 2)	**HB3**	63%
1b·dme	*p*-F-PhC≡N (n = 2)	**HB3**	≥95%
1c·dme	*p*-F-PhC≡N (n = 2)	**HB3**	≥95%
1d·dme	*p*-F-PhC≡N (n = 2)	**HB3**	≥95%
–	^{i}PrC≡N (n = 2)	**HB4**	0%
$MgBr_2$	^{i}PrC≡N (n = 2)	**HB4**	0%
1a	^{i}PrC≡N (n = 2)	**HB4**	39%
1b·dme	^{i}PrC≡N (n = 2)	**HB4**	≥95%
1c·dme	^{i}PrC≡N (n = 2)	**HB4**	≥95%
1d·dme	^{i}PrC≡N (n = 2)	**HB4**	≥95%
–	PhHC=NPh (n = 1)	**HB5**	0%
$MgBr_2$	PhHC=NPh (n = 1)	**HB5**	0%
1a	PhHC=NPh (n = 1)	**HB5**	66%
1b·dme	PhHC=NPh (n = 1)	**HB5**	76%
1c·dme	PhHC=NPh (n = 1)	**HB5**	66%
1d·dme	PhHC=NPh (n = 1)	**HB5**	60%
–	PhHC=NMe (n = 1)	**HB6**	19%
$MgBr_2$	PhHC=NMe (n = 1)	**HB6**	19%
1a	PhHC=NMe (n = 1)	**HB6**	79%
1b·dme	PhHC=NMe (n = 1)	**HB6**	70%
1c·dme	PhHC=NMe (n = 1)	**HB6**	72%
1d·dme	PhHC=NMe (n = 1)	**HB6**	54%

[a] Conditions: C_6D_6 ($MgBr_2$ in thf); room temperature or 333 K; 24 h; 5 mol% catalyst loading.

boration of phenyl and *tert*-butyl alkyne with equimolar amounts of pinacolborane was carried out at 333 K for 24 h. The reactions gave conversions of 62% to 88%, under selective formation of the anti-Markovnikov *syn*-product. For comparison, Ma and coworkers reported the application of a β-diketiminate magnesium complex in the catalytic hydroboration of terminal alkynes. The authors used 5 mol% of catalyst loading and temperatures above 373 K to obtain 99% conversion after six hours,[72] and Cavallo, Rueping and coworkers utilize 7 mol% of dibutylmagnesium as a precatalyst and obtained 83% conversion after 18 hours at 353 K in the hydroboration of terminal alkynes.[74] Thus, *ansa*-half-sandwich magnesium complexes **1a–d** operate at comparable temperatures. Subsequently, the hydroboration of nitriles and imines were investigated and found to be feasible at room temperature. With a catalyst loading of 5 mol%, conversions of up to 76% to ≥95% were achievable after 24 h at room temperature, depending on the catalyst. Noteworthy, magnesium complex **1a**, carrying the non-methylated Cp ring, performed significantly poorer in some of these reactions, possibly due to lower stability and corresponding catalyst degradation. Overall, the catalytic performance in these hydroboration reactions is remarkable for a magnesium-based system, as some other systems use higher catalyst loadings of 10 mol%,[72,75] while also requiring elevated temperatures of 333 K to 343 K.[33,36–38,72,75,76] However, an exception worth mentioning is a magnesium-based system reported by Hill and coworkers, which operates in a temperature range between 298 K and 343 K and gives high conversions within under 1 h in some cases.[73] Noteworthy, control experiments under identical conditions but without any metal compound or using 5 mol% of $MgBr_2$ showed little to no conversions (Table 3).

Different mechanisms for metal catalyzed hydroborations have been proposed in the literature. These often involve B–H oxidative addition to the metal center of the catalyst. However, in case of a magnesium(II) compound, this is not plausible. More likely, **1a–d** act as Lewis acids, activating the B–H moiety.[72,75,77] The Lewis acidic magnesium center may coordinate the pinacolborane *via* one of the oxygen atoms, while formation of a Mg–H–B multicenter bonding interaction activates the B–H bond and enables the transfer to the unsaturated C≡C/C≡N/C=N moieties (Scheme 5).

Hydroamination

Following these promising results in hydroboration catalysis, we expanded our investigations of hydroelementation catalysis to other *p*-block element hydrides and targeted hydroaminations. The well-known intramolecular hydroamination of α-ω-aminoalkenes is of great importance for the synthesis of *N*-heterocycles and has therefore been investigated extensively in the past decades, but still represents a challenge for metal catalysis, especially for *s*-block-based catalyst systems.[78–80]

When 2,2-diphenyl-4-penten-1-amine is treated with 10 mol% of **1a–d** at 323 K for 24 h, full conversion (≥95%) to

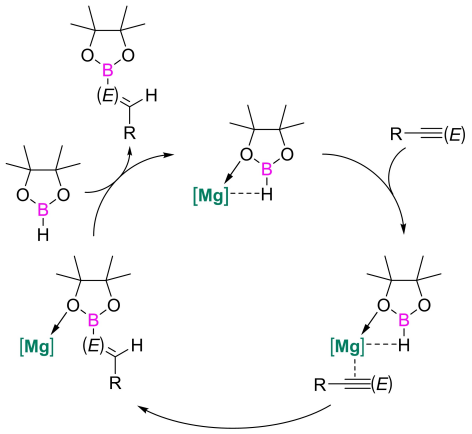

Scheme 5. Proposed mechanism for the hydroboration of alkynes and nitriles catalyzed by **1a–d** ((*E*)=CH, N).

the intramolecular hydroamination product is observed (Scheme 6).

Higher catalyst loading of 10 mol% and elevated temperatures are not unusual for this reaction and are commonly reported in the literature. For instance, Sadow and coworkers used loading of 10 mol% of magnesium-based catalysts, which gave quantitative conversion in the intramolecular hydroamination of 2,2-diphenyl-4-penten-1-amine after 1 h to 24 h at temperatures of room temperature and 323 K to 333 K.[43–45] Cano and coworkers had reported a related *ansa*-half-sandwich magnesium complex, that catalyzed the ring-closing hydroamination of 2,2-diphenyl-4-penten-1-amine at 333 K,[13] and Hultzsch and coworkers reported this hydroamination at room temperature using different magnesium based catalysts.[39–42] Furthermore, it must also be mentioned that Harder and coworkers have reported some highly active magnesium catalysts for this reaction, giving quantitative conversions after 45 min to 12 h at room temperature.[46,47] Their reported calcium-complex is even more efficient, as it needs only five minutes to reach full conversions.[47] Never the less, **1 a–d** performed quite competitively for a magnesium-based system.

Interestingly, the higher catalyst loading of 10 mol% enables an NMR characterization of the magnesium complexes in the catalytic reaction mixture. Most significantly, after the catalytic transformation is complete, the *ansa*-half-sandwich complexes **1 a–d** are intact, as for instance indicated by the typical resonances for the Si–C$\underline{H}_3$, N–C(C$\underline{H}_3$)$_3$ and Cp–$\underline{H}$ groups in case of **1 a** (Figure S13). This is an important finding, as it clearly indicates that **1 a–d** are most likely catalysts and not just precatalysts. Mechanistically, we assume that a bis(amine) complex – as discussed before (*vide infra*) – forms and that by dissociation of one of the amines and coordination/activation of the C=C double bond moiety, the N–H transfer can occur in the coordination sphere of the magnesium atom (Scheme 7). Such a mechanism was proposed for the intramolecular hydroamination by alkaline-earth metal complexes by Tobisch, backed up by DFT calculations.[81]

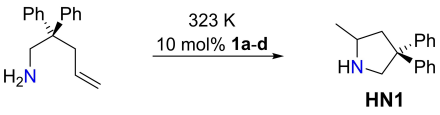

Scheme 6. Ring-closing hydroamination of 2,2-diphenyl-4-penten-1-amine to 2-methyl-4,4-diphenylpyrrolidine catalyzed by **1 a–d**.

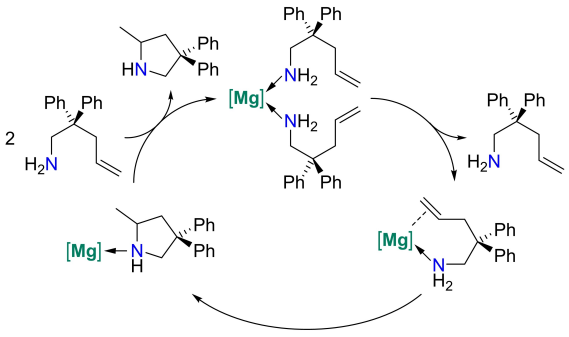

Scheme 7. Proposed mechanism for the cyclic hydroamination of 2,2-diphenyl-4-penten-1-amine to 2-methyl-4,4-diphenylpyrrolidine catalyzed by **1 a–d**.

Hydroacetylenation

Following the promising results of **1 a–d** in different dehydrocoupling and hydroelementation scenarios, we also investigated their catalytic abilities in the addition of terminal alkynes to carbodiimides, as this C–H activation/C–C bond formation reaction could in principle also be regarded as a type of hydroelementation (hydrocarboration). A catalyst loading of 5 mol% of **1 a–d** yielded 54% to 62% conversion after 24 h at 333 K, for the reaction of phenylacetylene with *N,N′*-dicyclohexylcarbodiimide. Changing the carbodiimide to *N,N′*-diisopropylcarbodiimide gave 60% to 80% at the same reaction conditions (Scheme 8; Table 4). **1 a–d** all performed relatively equally in these transformations.

For comparison, Coles and coworkers reported of a magnesium compound, that promoted the catalytic addition of phenylacetylene to *N,N′*-diisopropylcarbodiimide, giving conversions of ca. 50% after 24 h at 323 K.[48] This is somewhat comparable to the catalytic performance of **1 a–d**. Noteworthy however, Hill and coworkers reported a magnesium compound that was able to catalyze this reaction at room temperature, with conversions in the range of 60% after 24 h. Furthermore, some heavier alkaline earth metal compounds have been shown to possess an even higher catalytic activity.[49]

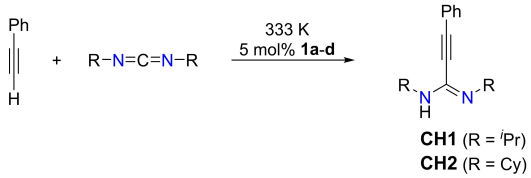

Scheme 8. Hydroacetylenation of phenylacetylene and carbodiimides catalyzed by **1 a–d**.

Table 4. Summary of catalysts, substrates, formed products and conversions of the hydroacetylenation reactions catalyzed by **1 a–d**, corresponding to Scheme 8.[a]

catalyst	substrate + PhC≡CH	product	Conversion
1 a	^{i}PrN=C=N^{i}Pr	CH1	79%
1 b·dme	^{i}PrN=C=N^{i}Pr	CH1	73%
1 c·dme	^{i}PrN=C=N^{i}Pr	CH1	78%
1 d·dme	^{i}PrN=C=N^{i}Pr	CH1	63%
1 a	CyN=C=NCy	CH2	62%
1 b·dme	CyN=C=NCy	CH2	54%
1 c·dme	CyN=C=NCy	CH2	61%
1 d·dme	CyN=C=NCy	CH2	56%

[a] Conditions: C_6D_6; 333 K; 24 h; 5 mol% catalyst loading.

We assume that a similar mechanism is in operation for **1 a–d** as was previously described by Coles *et al.* and Hill *et al.* for their systems (Scheme 9).[48,49,82]

Following coordination of the carbodiimide to the electrophilic magnesium center, the phenylacetylene may coordinate to the magnesium center as well and then undergo the addition reaction upon C–H activation in the coordination sphere of the magnesium center. Noteworthy, the stoichiometric reaction of **1 b**·(dme) with *N,N'*-diisopropylcarbodiimide resulted in the formation of the postulated complex, along uncoordinated dme, as indicated by $^{1}H/^{13}C\{^{1}H\}/^{29}Si\{^{1}H\}$ NMR spectroscopy and importantly, no free ligand was detected,[60] suggesting that **1 a–d** are catalysts for this reaction and not just precatalysts.

Conclusion

In this work, we reported the syntheses and characterization of four constrained geometry *ansa*-half-sandwich complexes of magnesium, **1 a–d**. We used these compounds as homogenous catalysts in different high atom economy scenarios, more specifically dehydrocoupling and hydroelementation transformations, including B–N and Si–N (cross-) dehydrocoupling, hydroborations, hydroaminations and hydroacetylenations. In amine-borane dehydrocoupling, as well as in amine silane cross-dehydrocoupling, **1 a–d** are among the best magnesium-based systems, as they operate at room temperature and generally give high conversions after short reaction times. In hydroboration reactions, these compounds have also been found to be useful catalysts that can readily catalyze the hydroboration of multiple substrates, such as alkynes, nitriles and imines. Furthermore, we could also successfully use **1 a–d** in the ring-closing hydroamination of an α-ω-aminoalkene. Finally, their catalytic capabilities in the addition of a terminal alkyne to carbodiimides was demonstrated.

Thus, this work significantly expands the field of application of cyclopentadienyl magnesium compounds in homogenous catalysis, reporting a new kind of magnesium catalyst that possesses a broad application scope in different catalytic transformations.

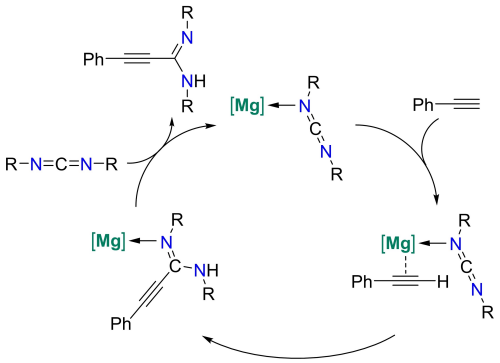

Scheme 9. Proposed mechanism for the hydroacetylenation of phenylacetylene and carbodiimides catalyzed by **1 a–d**.

Experimental Section

General Details

All manipulations were carried out under an argon inert gas atmosphere (argon 5.0), using either Schlenk line techniques or a glovebox. NMR spectra were recorded on Bruker Avance III 300 and Bruker Avance III 400 spectrometers. ^{1}H and ^{13}C NMR spectra were referenced using the solvent signals ($\delta^{1}H$ ($CHCl_3$) = 7.26, $\delta^{1}H$ (C_6HD_5) = 7.16, $\delta^{1}H$ (thf-d7) = 3.58; $\delta^{13}C$ (C_6D_6) = 128.06, $\delta^{13}C$ ($CDCl_3$) = 77.16, $\delta^{13}C$ (thf-d8) = 67.57). ^{11}B and ^{29}Si NMR spectra were referenced using external standards ($\delta^{11}B$ ($BF_3 \cdot OEt_2$) = 0, $\delta^{29}Si$ ($SiMe_4$) = 0). Crystal structures have been deposited with the Cambridge Crystallographic Data Centre (CCDC) and are available free of charge from the Cambridge Structural Database (reference numbers: 2193652, 2193656, 2193657, 2193660, 2193661).

Synthesis and Characterization of Magnesium Complexes 1 a–d

1 a

To a solution of $(C_5H_5)SiMe_2NHtBu$ (4.19 g, 21.4 mmol) in hexane (~125 mL) precooled to 273 K was added a solution of *n*-butyl-*sec*-butylmagnesium (0.7 M in hexane, 30.1 mL, 21.1 mmol). The cooling bath was removed, and the mixture was heated to 333 K for 20 h. The precipitated product was isolated by filtration and dried *in vacuo* to obtain **1 a** as colorless solid. Yield: 4.04 g/88 %.

^{1}H NMR (400.13 MHz, thf-d_8): δ (in ppm): 6.13 (t, $^{3}J_{HH}$ = 2.3 Hz, 2 H; Cp-*H*), 5.99 (t, $^{3}J_{HH}$ = 2.3 Hz, 2 H; Cp-*H*), 1.04 (s, 9 H; $C(CH_3)_3$), 0.25 (s, 6 H; Si-CH_3); $^{13}C\{^{1}H\}$ NMR (100.62 MHz, thf-d_8): δ (in ppm): 117.5 (Cp), 111.4 (Cp), 108.8 (Cp), 51.6 ($C(CH_3)_3$), 37.9 ($C(CH_3)_3$), 4.7 (Si-CH_3); $^{29}Si\{^{1}H\}$ NMR (79.49 MHz, thf-d_8): δ (in ppm): −22.6.

1 b·dme

To a solution of $(C_5Me_4H)SiMe_2NHtBu$ (4.42 g, 17.6 mmol) in hexane (~125 mL) was added a solution of *n*-butyl-*sec*-butylmagnesium (0.7 M in hexane, 25.1 mL, 17.6 mmol). The mixture was stirred for two days at 333 K and subsequently 2 days at room temperature. The solvent was removed *in vacuo* to give a yellow oil. The oil was diluted with dme and stored at 248 K to obtained **1 b**·dme as colorless crystals. Yield: 1.96 g/31 %.

^{1}H NMR (400.13 MHz, thf-d_8): δ (in ppm): 3.42 (dme), 3.27 (dme), 2.13 (s, 6 H, Cp-CH_3), 1.94 (s, 6 H, Cp-CH_3), 1.09 (s, 9 H, $C(CH_3)_3$), 0.32 (s, 6 H, Si-CH_3); $^{13}C\{^{1}H\}$ NMR (100.62 MHz, thf-d_8): δ (in ppm): 116.6 (Cp), 114.4 (Cp), 108.3 (Cp), 72.8 (dme), 59.0 (dme), 51.5 ($C(CH_3)_3$), 38.0 ($C(CH_3)_3$), 15.0 (Cp-CH_3), 12.2 (Cp-CH_3), 8.9 (Si-CH_3); $^{29}Si\{^{1}H\}$ NMR (79.49 MHz, thf-d_8): δ (in ppm): −22.1.

1 c·dme

To a solution of $(C_5Me_4H)SiPh_2NHtBu$ (7.89 g, 21.0 mmol) in hexane (~125 mL) and dme (~5 mL) was added a solution of *n*-butyl-*sec*-butylmagnesium (0.7 M in hexane, 30.0 mL, 21.0 mmol). The mixture was stirred for one day at 333 K. The precipitated product was isolated by filtration as a pale-yellow solid and dried *in vacuo*. Yield: 3.06 g/30 %.

^{1}H NMR (400.13 MHz, thf-d_8): δ (in ppm): 7.78-7.71 (m, 4 H, Ph-*H*), 7.17-7.07 (m, 6 H, Ph-*H*), 3.42 (dme), 3.27 (dme), 1.93 (s, 6 H, Cp-CH_3), 1.67 (s, 6 H, Cp-CH_3), 1.30 (s, 9 H, $C(CH_3)_3$); $^{13}C\{^{1}H\}$ NMR (100.62 MHz, thf-d_8): δ (in ppm): 148.1 (Ph), 137.6 (Ph), 136.4 (Ph), 127.4 (Ph), 127.1 (Ph), 118.4 (Cp), 115.0 (Cp), 105.3 (Cp), 72.8 (dme),

59.0 (dme), 51.5 ($C(CH_3)_3$), 38.5 ($C(CH_3)_3$), 15.2 (Cp-CH_3), 12.3 (Cp-CH_3); $^{29}Si\{^1H\}$ NMR (79.49 MHz, thf-d_8): δ (in ppm): −30.8.

1 d·dme

To a solution of $(C_5Me_4H)SiMe_2NHPh$ (4.37 g, 20.3 mmol) in toluene (~100 mL) and dme (~5 mL) was added a solution of *n*-butyl-*sec*-butylmagnesium (0.7 M in hexane, 29.0 mL, 20.3 mmol). The mixture was stirred for one day at 333 K. The precipitated crude product was isolated by filtration and dried *in vacuo*. The crude product was diluted with dme and the solution was stored at 248 K to obtain the product as colorless crystals. Yield: 1.05 g/16%.

^1H NMR (400.13 MHz, thf-d_8): δ (in ppm): 6.74-6.68 (m, 2 H, Ph-*H*), 6.20-6.16 (m, 2 H, Ph-*H*), 6.09-6.04 (m, 1 H, Ph-*H*), 3.42 (dme), 3.27 (dme), 2.14 (s, 6 H, Cp-CH_3), 2.01 (s, 6 H, Cp-CH_3), 0.52 (s, 6 H, Si-CH_3); $^{13}C\{^1H\}$ NMR (100.62 MHz, thf-d_8): δ (in ppm): 159.4 (Ph), 129.1 (Ph), 116.4 (Ph), 116.2 (Cp), 111.7 (Cp), 109.1 (Cp), 72.8 (dme), 59.1 (dme), 14.6 (Cp-CH_3), 12.0 (Cp-CH_3), 4.0 (Si-CH_3); $^{29}Si\{^1H\}$ NMR (79.49 MHz, thf-d_8): δ (in ppm): −17.7.

Acknowledgements

Support and funding by the Deutsche Forschungsgemeinschaft, DFG, (Emmy Noether program SCHA1915/3-1/2) is gratefully acknowledged. Instrumentation and technical assistance for this work were provided by the Service Center X-ray Diffraction, with financial support from Saarland University and the Deutsche Forschungsgemeinschaft (INST 256/506-1). Open Access funding enabled and organized by Projekt DEAL.

Conflict of Interest

The authors declare no conflict of interest.

Data Availability Statement

The data that support the findings of this study are available in the supplementary material of this article.

Keywords: Magnesium · half-sandwich complexes · constrained geometry complexes · dehydrocoupling · hydroelementation

[1] P. J. Shapiro, E. Bunel, W. P. Schaefer, J. E. Bercaw, *Organometallics* **1990**, *9*, 867–869.
[2] W. E. Piers, P. J. Shapiro, E. E. Bunel, J. E. Bercaw, *Synlett* **1990**, *1990*, 74–84.
[3] J. Okuda, *Chem. Ber.* **1990**, *123*, 1649–1651.
[4] M. C. Baier, M. A. Zuideveld, S. Mecking, *Angew. Chem. Int. Ed.* **2014**, *53*, 9722–9744; *Angew. Chem.* **2014**, *126*, 9878–9902.
[5] J. Cano, K. Kunz, *J. Organomet. Chem.* **2007**, *692*, 4411–4423.
[6] A. L. McKnight, R. M. Waymouth, *Chem. Rev.* **1998**, *98*, 2587–2598.
[7] H. Braunschweig, F. M. Breitling, *Coord. Chem. Rev.* **2006**, *250*, 2691–2720.
[8] J. M. Pietryga, J. D. Gorden, C. L. B. Macdonald, A. Voigt, R. J. Wiacek, A. H. Cowley, *J. Am. Chem. Soc.* **2001**, *123*, 7713–7714.
[9] R. J. Wiacek, C. L. B. Macdonald, J. N. Jones, J. M. Pietryga, A. H. Cowley, *Chem. Commun.* **2003**, 430–431.
[10] M. Weger, P. Pahl, F. Schmidt, B. S. Soller, P. J. Altmann, A. Pöthig, G. Gemmecker, W. Eisenreich, B. Rieger, *Macromolecules* **2019**, *52*, 7073–7080.
[11] I.-A. Bischoff, B. Morgenstern, A. Schäfer, *Chem. Commun.* **2022**, *58*, 8934–8937.
[12] T. K. Panda, C. G. Hrib, P. G. Jones, J. Jenter, P. W. Roesky, M. Tamm, *Eur. J. Inorg. Chem.* **2008**, *2008*, 4270–4279.
[13] C. Gallegos, R. Camacho, M. Valiente, T. Cuenca, J. Cano, *Catal. Sci. Technol.* **2016**, *6*, 5134–5143.
[14] M. Magre, M. Szewczyk, M. Rueping, *Chem. Rev.* **2022**, *122*, 8261–8312.
[15] R. Rochat, M. J. Lopez, H. Tsurugi, K. Mashima, *ChemCatChem* **2016**, *8*, 10–20.
[16] M. M. D. Roy, A. A. Omaña, A. S. S. Wilson, M. S. Hill, S. Aldrige, E. Rivard, *Chem. Rev.* **2021**, *121*, 12784–12965.
[17] D. L. Anderson, in *Chemical Composition of the Mantle (Chapter 8), Theory of the Earth*, Blackwell Scientific, Boston, **1989**, pp. 147–175.
[18] P. Nuss, M. J. Eckelman, *PLoS One* **2014**, *9*, e101298.
[19] B. Peng, J. Chen, *Energy Environ. Sci.* **2008**, *1*, 479–483.
[20] M. B. Reuter, K. Hageman, R. Waterman, *Chem. Eur. J.* **2021**, *27*, 3251–3261.
[21] M. Arrowsmith, in:Dehydrocoupling, *Other Cross-couplings (Chapter 9), Early Main Group Metal Catalysis: Concepts and Reactions* (Edl: S. Harder), Wiley-VCH, Weinheim, **2020**, pp. 225–250.
[22] E. M. Leitao, T. Jurca, I. Manners, *Nat. Chem.* **2013**, *5*, 817–829.
[23] R. L. Melen, *Chem. Soc. Rev.* **2016**, *45*, 775–788.
[24] L. Wirtz, W. Haider, V. Huch, M. Zimmer, A. Schäfer, *Chem. Eur. J.* **2020**, *26*, 6176–6184.
[25] L. Wirtz, J. Lambert, B. Morgenstern, A. Schäfer, *Organometallics* **2021**, *40*, 2108–2117.
[26] D. J. Liptrot, M. S. Hill, M. F. Mahon, D. J. MacDougall, *Chem. Eur. J.* **2010**, *16*, 8508–8515.
[27] M. S. Hill, M. Hodgson, D. J. Liptrot, M. F. Mahon, *Dalton Trans.* **2011**, *40*, 7783–7790.
[28] P. Bellham, M. D. Anker, M. S. Hill, G. Kociok-Köhn, M. F. Mahon, *Dalton Trans.* **2016**, *45*, 13969–13978.
[29] A. C. A. Ried, L. J. Taylor, A. M. Geer, H. E. L. Williams, W. Lewis, A. J. Blake, D. L. Kays, *Chem. Eur. J.* **2019**, *25*, 6840–6846.
[30] J. F. Dunne, S. R. Neal, J. Engelkemier, A. Ellern, A. D. Sadow, *J. Am. Chem. Soc.* **2011**, *133*, 16782–16785.
[31] M. S. Hill, D. J. Liptrot, D. J. MacDougall, M. F. Mahon, T. P. Robinson, *Chem. Sci.* **2013**, *4*, 4212–4222.
[32] A. Baishya, T. Peddarao, S. Nembenna, *Dalton Trans.* **2017**, *46*, 5880–5887.
[33] I. Banerjee, T. K. Panda, *Appl. Organomet. Chem.* **2021**, *35*, e6333.
[34] S. Rej, A. Das, T. K. Panda, *Adv. Synth. Catal.* **2021**, *363*, 4818–4840.
[35] K. Watanabe, J. H. Pang, R. Takita, S. Chiba, *Chem. Sci.* **2022**, *13*, 27–38.
[36] D. Hayrapetyan, A. Y. Khalimon, *Chem. Asian J.* **2020**, *15*, 2575–2587.
[37] D. Mukherjee, S. Shirase, T. P. Spaniol, K. Mashima, J. Okuda, *Chem. Commun.* **2016**, *52*, 13155–13158.
[38] S. Schnitzler, T. P. Spaniol, J. Okuda, *Inorg. Chem.* **2016**, *55*, 12997–13006.
[39] P. Horrillo-Martínez, K. C. Hultzsch, *Tetrahedron Lett.* **2009**, *50*, 2054–2056.
[40] X. Zhang, T. J. Emge, K. C. Hultzsch, *Organometallics* **2010**, *29*, 5871–5877.
[41] X. Zhang, T. J. Emge, K. C. Hultzsch, *Angew. Chem. Int. Ed.* **2012**, *51*, 394–398; *Angew. Chem.* **2012**, *124*, 406–410.
[42] X. Zhang, S. Tobisch, K. C. Hultzsch, *Chem. Eur. J.* **2015**, *21*, 7841–7857.
[43] J. F. Dunne, D. B. Fulton, A. Ellern, A. D. Sadow, *J. Am. Chem. Soc.* **2010**, *132*, 17680–17683.
[44] S. R. Neal, A. Ellern, A. D. Sadow, *J. Organomet. Chem.* **2011**, *696*, 228–234.
[45] N. Eedugurala, M. Hovey, H.-A. Ho, B. Jana, N. L. Lampland, A. Ellern, A. D. Sadow, *Organometallics* **2015**, *34*, 5566–5575.
[46] B. Freitag, C. A. Fischer, J. Penafiel, G. Ballmann, H. Elsen, C. Färber, D. F. Piesik, S. Harder, *Dalton Trans.* **2017**, *46*, 11192–11200.
[47] P. C. Stegner, J. Eyselein, G. M. Ballmann, J. Langer, J. Schmidt, S. Harder, *Dalton Trans.* **2021**, *50*, 3178–3185.
[48] R. J. Schwamm, M. P. Coles, *Organometallics* **2013**, *32*, 5277–5280.
[49] M. Arrowsmith, M. R. Crimmin, M. S. Hill, S. L. Lomas, M. S. Heng, P. B. Hitchcock, G. Kociok-Köhn, *Dalton Trans.* **2014**, *43*, 14249–14256.
[50] H. G. Alt, K. Föttinger, W. Milius, *J. Organomet. Chem.* **1999**, *572*, 21–30.
[51] D. W. Carpenetti, L. Kloppenburg, J. T. Kupec, J. L. Petersen, *Organometallics* **1996**, *15*, 1572–1581.

[52] J. Pinkas, M. Horáček, V. Varga, K. Mach, K. Szarka, A. Vargová, R. Gyepes, *Polyhedron* **2020**, *188*, 114704.
[53] Z. Hou, T. Koizumi, M. Nishiura, Y. Wakatsuki, *Organometallics* **2001**, *20*, 3323–3328.
[54] a) C. Cremer, H. Jacobsen, P. Burger, *Chimia* **1997**, *51*, 650–653; b) C. Cremer, H. Jacobsen, P. Burger, *Chimia* **1997**, *51*, 968.
[55] P. Perrotin, P. J. Shapiro, M. Williams, B. Twamley, *Organometallics* **2007**, *26*, 1823–1826.
[56] P. Perrotin, B. Twamley, P. J. Shapiro, *Acta Crystallogr. Sect. E* **2007**, *63*, m1277-m1278.
[57] L. Wirtz, A. Schäfer, *Chem. Eur. J.* **2021**, *27*, 1219–1230.
[58] Fluoride ion affinities (FIA) were calculated according to a literature established method from the isodesmic reactions with Et_3B/Et_3BF^-. For more details see for example: H. Großekappenberg, M. Reißmann, M. Schmidtmann, T. Müller, *Organometallics* **2015**, *34*, 4952–4958.
[59] Global electrophilicity indices ω were calculated following the method of Stephan and coworkers (Method C): A. R. Jupp, T. C. Johnstone, D. W. Stephan, *Inorg. Chem.* **2018**, *57*, 14764–14771.
[60] See supporting information for further details.
[61] C. M. Vogels, P. E. O'Connor, T. E. Phillips, K. J. Watson, M. P. Shaver, P. G. Hayes, S. A. Westcott, *Can. J. Chem.* **2001**, *79*, 1898–1905.
[62] D. J. Liptrot, M. S. Hill, M. F. Mahon, A. S. S. Wilson, *Angew. Chem. Int. Ed.* **2015**, *54*, 13362–13365; *Angew. Chem.* **2015**, *127*, 13560–13563.
[63] A. Harinath, S. Anga, T. K. Panda, *RSC Adv.* **2016**, *6*, 35648–35653.
[64] S. Kaufmann, P. W. Roesky, *Eur. J. Inorg. Chem.* **2021**, *2021*, 2899–2905.
[65] A. G. M. Barrett, M. R. Crimmin, M. S. Hill, P. B. Hitchcock, P. A. Procopiou, *Organometallics* **2007**, *26*, 4076–4079.
[66] Z. Yang, M. Zhong, X. Ma, K. Nijesh, S. De, P. Parameswaran, H. W. Roesky, *J. Am. Chem. Soc.* **2016**, *138*, 2548–2551.
[67] J. D. Erickson, T. Y. Lai, D. J. Liptrot, M. M. Olmstead, P. P. Power, *Chem. Commun.* **2016**, *52*, 13656–13659.
[68] Y. Wang, P. Xu, X. Xu, *Chin. Chem. Lett.* **2021**, *32*, 4002–4005.
[69] E. A. Romero, J. L. Peltier, R. Jazzar, G. Bertrand, *Chem. Commun.* **2016**, *52*, 10563–10565.
[70] C. Bellini, J.-F. Carpentier, S. Tobisch, Y. Sarazin, *Angew. Chem. Int. Ed.* **2015**, *54*, 7679–7683; *Angew. Chem.* **2015**, *127*, 7789–7793.
[71] C. Bellini, V. Dorcet, J.-F. Carpentier, S. Tobisch, Y. Sarazin, *Chem. Eur. J.* **2016**, *22*, 4564–4583.
[72] J. Li, M. Luo, X. Sheng, H. Hua, W. Yao, S. A. Pullarkat, L. Xu, M. Ma, *Org. Chem. Front.* **2018**, *5*, 3538–3547.
[73] M. Arrowsmith, M. S. Hill, G. Kociok-Köhn, *Chem. Eur. J.* **2013**, *19*, 2776–2783.
[74] M. Magre, B. Maity, A. Falconnet, L. Cavallo, M. Rueping, *Angew. Chem. Int. Ed.* **2019**, *58*, 7025–7029; *Angew. Chem.* **2019**, *131*, 7099–7103.
[75] C. Weetman, M. D. Anker, M. Arrowsmith, M. S. Hill, G. Kociok-Köhn, D. J. Liptrot, M. F. Mahon, *Chem. Sci.* **2016**, *7*, 628–641.
[76] K. Manna, P. Ji, F. X. Greene, W. Lin, *J. Am. Chem. Soc.* **2016**, *138*, 7488–7491.
[77] M. R. Crimmin, M. S. Hill, in *Homogeneous Catalysis with Organometallic Complexes of Group 2*, *Topics in Organometallic Chemistry*, Springer, Berlin Heidelberg, **2013**, pp. 191–242.
[78] T. E. Müller, K. C. Hultsch, M. Yus, F. Foubelo, M. Tada, *Chem. Rev.* **2008**, *108*, 3795–3892.
[79] L. Huang, M. Arndt, K. Gooßen, H. Heydt, L. J. Gooßen, *Chem. Rev.* **2015**, *115*, 2596–2697.
[80] J. Huo, G. He, W. Chen, X. Hu, Q. Deng, D. Chen, *BMC Chem. Biol.* **2019**, *13*, 89.
[81] S. Tobisch, *Chem. Eur. J.* **2015**, *21*, 6765–6779.
[82] R. J. Schwamm, B. M. Day, N. E. Mansfield, W. Knowelden, P. B. Hitchcock, M. P. Coles, *Dalton Trans.* **2014**, *43*, 14302–14314.

Manuscript received: August 9, 2022
Revised manuscript received: September 20, 2022
Version of record online: October 26, 2022